

High-Float Emulsion Residue: A New Rheological Model Based on the
Existence of a Yield Stress

by

Justin Philip Suda

A thesis submitted in partial fulfillment of the requirements for the degree of

Master of Science

in

Chemical Engineering

Department of Chemical and Materials Engineering

University of Alberta

© Justin Philip Suda, 2016

Abstract

“High-float” (HF) emulsions are dispersions of micron-sized bitumen droplets in water, with a special type of anionic surfactant functioning as stabilizer. By allowing the water to evaporate from an HF emulsion, what remains is called a “high-float emulsion residue.” Although indistinguishable in appearance from the original bitumen, the HF emulsion residue possesses rheological properties that are remarkably different from those of bitumen. In particular, the HF residue exhibits a yield stress which prevents it from draining under the influence of gravity even at elevated temperatures. In this study, a new rheological model is proposed for the HF emulsion residue. An experimental procedure is also introduced to measure the yield stress using dynamic shear rheometry.

Preface

The research conducted for this thesis was part of a collaboration between the University of Alberta, led by Dr. Anthony Yeung, and Justin Suda from Gecan (a division of Canadian Road Builders). Dr. Yeung was the supervisory author involved with theoretical application, experimental microscopic techniques, and data analysis. This thesis is an original work by Justin Suda.

Dedication

My dissertation is dedicated to my loving wife and two boys. Without their understanding and patience, this work would have never been accomplished.

Table of Contents

Chapter 1: Introduction	1
Chapter 2: Principles of Rheology — A Brief Summary	15
Chapter 3: Materials and Methods	34
Chapter 4: Results and Discussions	39
Chapter 5: Conclusions and Future Work.....	47

List of Figures

Figure 1.1 Asphalt concrete

Figure 1.2 Example of a pavement preservation application called “chip sealing”

Figure 1.3 Microscope image of a bitumen emulsion

Figure 1.4 “Bleeding”

Figure 1.5 The float test (ASTM D139)

Figure 1.6 Flow behaviours of bitumen and a high-float emulsion residue

Figure 1.7 Mayonnaise with inherent yield stress

Figure 2.1 An elemental volume of material under pure shear

Figure 2.2 Front views of the material element before and after pure shear deformation

Figure 2.3 One dimensional metaphors of elastic solids and viscous fluids

Figure 2.4 Representation of a Kelvin-Voigt material

Figure 2.5 Representation of a Maxwell material

Figure 2.6 The two possible forms of the elastic function $\sigma_e(\varepsilon)$

Figure 2.7 Steady state relation between $\sigma(t)$ and $\varepsilon(t)$ when a material is subjected to sinusoidal excitation (with period T)

Figure 2.8 Variations of the apparent viscosity μ_{app} with applied stress σ

Figure 2.9 Simple algorithm for calculating the response of a material to stress-ramp excitation

Figure 2.10 Setup of the dynamic shear rheometer (DSR)

Figure 3.1 Colloidal mill

Figure 3.2 Residue-by-distillation set up

Figure 4.1 Variation of phase angle (i.e. $\tan \delta$) with the frequency of oscillation

Figure 4.2 Variation of the shear modulus $|G^*|$ with the frequency of oscillation

Figure 4.3 Stress-ramp data of the three binder materials

Figure 4.4 Numerical simulation of stress-ramp response according to equation 2.11

Figure 4.5 Numerical simulation of stress-ramp response according to equations 2.12b

Chapter 1: Introduction

This research is motivated by the engineering practice known as pavement construction and preservation. Despite the first impression that this may invoke, the basic principles which underlie such an application belong very much in the realm of chemical engineering science. The title of this thesis contains a number of technical terms which will be clarified in this chapter. To begin, an *emulsion*, in the present context, is a suspension of micron-sized bitumen droplets in an aqueous medium. (Here, “bitumen” refers to the by-product which results from the distillation of crude oil in refineries. This substance is very similar — although not identical — to the naturally-occurring bitumen that is found in the Athabasca oil sands. In the United States, bitumen that is used for road construction is often called “asphalt.”) In regard to pavement construction and preservation, bitumen emulsions are playing an increasingly important role; one may in fact assert that these emulsion systems represent the future of pavement preservation. Before describing the specific function of bitumen emulsions in road construction, I will first provide some general background on this particular engineering practice.

1.1 Pavement Preservation in Canada

Pavement preservation refers to the engineering practice that is aimed at increasing the life expectancy of road structures. In Canada, the network of paved public roads for two-lane-equivalent traffic is in excess of 400 thousand kilometers (Transport Canada, 2016); to put this in perspective, it is ten times the Earth’s circumference. In addition to enduring increasing traffic volumes, this vast road network is also exposed to some of the most extreme weather conditions: road surface temperatures in Canada can vary from -50°C in the winter to 80°C in the summer. As a result of these natural and man-made factors, the roads are deteriorating to the extent of

becoming unravelled, cracked, or heaved; they will require total reconstruction if surface preservation treatments were not made in time.

Pavement preservation techniques normally involve reinforcing distressed road surfaces with layers of “asphalt concrete.” Asphalt concrete, similar to cement concrete, is a composite material consisting of a matrix of “aggregates” (rocks of selected sizes) that are held together by a glue — or “binder” — which is ideally a viscoelastic material. As is well known, bitumen is the material of choice as a binder. An illustration of an asphalt concrete is shown in Figure 1.1.

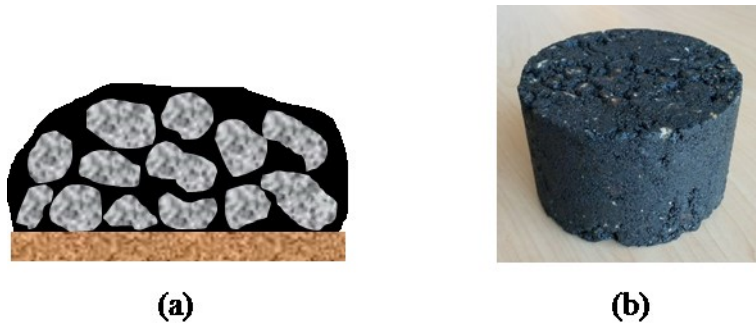


Figure 1.1 Asphalt concrete, which consists of a matrix of “aggregates” (rocks of a chosen size range) held together by a glue or “binder” (bitumen). (a) Simple sketch of an asphalt concrete; (b) actual photograph.

During formation of an asphalt concrete, it is clear that the binder material (bitumen) must undergo very significant changes to its mechanical properties: it must, for a temporary period, be able to flow freely so that it can occupy the void spaces between the aggregates. Since bitumen is naturally very viscous, its viscosity must first be drastically reduced. There are three ways of “liquefying” the bitumen binder; these are (a) increasing its temperature, (b) diluting it with a volatile solvent, or (c) emulsifying the bitumen in water. A greatly simplified description of pavement preservation procedures is as follows: the aggregates and the “liquefied” binder are first laid down on a distressed road; the composite is then compacted down to a smooth surface; and finally, the binder is allowed to *cure*, i.e. to regain its original mechanical strength.

Perhaps the most obvious (and historically the first) method of reducing bitumen viscosity by heating. Such a process, also called hot mix asphalt (HMA), is known to be robust, reliable, but is also extremely energy intensive. During operation, the bitumen must be heated to 160°C or higher for it to flow freely (at these temperatures, the viscosity of bitumen is similar to that of water). In an HMA process, curing is achieved by simply allowing the bitumen cool to ambient temperature, thereby regaining its viscosity (and often its viscoelasticity). The second method of viscosity reduction is by diluting the bitumen with petroleum solvents such as naphtha or kerosene; the resulting diluted bitumen is sometimes called a “cutback asphalt.” Curing of a cutback involves allowing the volatile solvent to vaporize and the bitumen to regain its original properties. From an environmental perspective, there are clear drawbacks associated with both the HMA and cutback approaches. The first method suffers from excessive energy requirement, while the second method involves the release of volatile organic compounds (VOCs) into the atmosphere. In Canada, the federal government (Environment and Climate Change Canada) is beginning to impose much stricter regulations on the road construction industry in regard to VOC emissions. In view of the drawbacks associated with heating or diluting with volatile solvents, the third method of “liquefying” the bitumen binder, through emulsification, is becoming a much preferred choice.

Emulsification is the most economic and environmentally responsible way of liquefying the bitumen binder. The basic idea of this process is simple: since water is far less viscous than bitumen under normal (ambient) conditions, and since the two materials are immiscible, it seems sensible to break up the much “harder” binder into small droplets (typically microns in size) and use water as the carrier fluid. The resulting system is what is known as an *oil-in-water emulsion*. Forming a bitumen emulsion, however, requires more than just bitumen and water. As is well-

known in colloid science, an emulsion — whether oil-in-water or water-in-oil — cannot be formed, and maintained, without addition of an emulsifying agent, which is often a surfactant. (The surfactant lowers the bitumen-water interfacial tension, which facilitates the emulsification process. After an emulsion is formed, the surfactant is also responsible for preventing the bitumen droplets from coalescing, which leads to the “breaking” of the emulsion.) With water as the continuous phase, the suspension flows easily and can be laid down with the aggregates (the rocks) during pavement preservation operations. Figure 1.2 shows such an operation.



Figure 1.2 Example of a pavement preservation application called “chip sealing.” The white truck in front first sprays a layer of bitumen emulsion (approx. 2 mm in thickness) onto the distressed pavement; it is closely followed by a second truck which deposits aggregates (small rocks) onto the sprayed emulsion layer. Trailing behind at a greater distance is a roller truck for compacting the composite structure.

The curing of an emulsified binder involves simply allowing the water to evaporate; what remains after evaporation of the water is called an *emulsion residue* (another technical term which appears in the title of this thesis). The conventional belief is that the evaporation of water will bring together all bitumen droplets, cause them to coalesce and thus recover the original

bitumen — complete with all of its viscoelastic properties. Stated another way, the emulsion residue, which now functions as the binder for the aggregates, is often assumed to be identical to the original bitumen. However, it should be noted that the third component of a bitumen emulsion — the emulsifier — also remains in the residue. It is possible that the presence of the emulsifier in the residue can have unintended — and sometimes desirable — effects on the mechanical properties of the residue. (The type of bitumen emulsion examined in this thesis, the so-called “high-float emulsion,” is an important example. More details on this emulsion system will appear in Section 1.4.) Thus, although an emulsion residue is indistinguishable from the original bitumen by appearance, its rheological properties (i.e. how it deforms and flows) can in some cases be quite different. In summary, compared to the hot mix and cutback approaches (i.e. liquefying the bitumen with heat or by solvent dilution), not only is emulsification a more cost effective and environmentally responsible alternative, it also has the potential of providing the emulsion residue — which is now the binder material — with unique rheological properties that cannot be replicated in the original bitumen system.

1.2 Brief History of Bitumen Emulsions

Bitumen emulsions were first introduced in the 1920s, most notably by H.A. MacKay with his 1922 patent (McNichol 2005). These emulsions were first applied as dust and spray seal coatings in the paving industry, and had since been extended to an increasingly wider range of applications for constructing and maintaining road infrastructures. In 1930, a survey article was published (*Scientific American* 1930) in which the author observed that bitumen emulsion usage had expanded beyond road paving and into other applications such as moisture proofing, flooring, and protective coatings on structural steel and pipelines. Also evident in the article was a deeper understanding of the emulsifiers (e.g. clays, soaps, and even ox-blood in the early days),

and how they facilitated dispersion of bitumen in water. However, the article also mentioned that road emulsions, once applied, required a 48-hour period to “set” before heavy vehicles could be allowed to roll over them. This indicated that the technology surrounding the curing rate of emulsions had not yet evolved. Over the next four decades, bitumen emulsions showed slow but steady growth as road builders began to understand their various benefits (e.g. cost effectiveness and environmental performance), and how they may be an alternative to traditional HMA (hot mix asphalt) technology. Interests in HMA peaked after World War II with the sharp increases in heavy volume traffic, which demanded reliable and proven methods of creating road infrastructures with little regard, at that time, to the energy cost. It was not until the energy crisis in the 1970s (oil embargos in the Middle East) that interests in bitumen emulsion systems were renewed. Soon following this economic driver, there were also increasing concerns with the environmental performance of the pavement industry. This movement encouraged the reduction of atmospheric pollution and energy consumption, and it continues to this day. And present, with evolving technology and improved performance, there is a growing demand for bitumen emulsions in all road applications.

1.3 Components of Bitumen Emulsions

Figure 1.3 shows a microscope image of a bitumen emulsion:

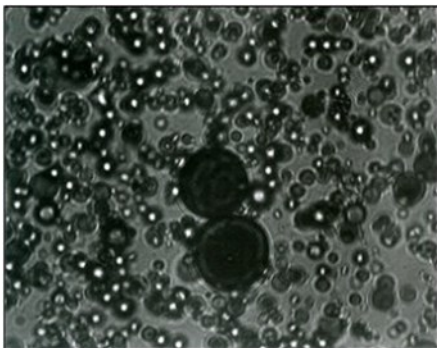


Figure 1.3 Microscope image of a bitumen emulsion, which is a suspension of bitumen droplets in an aqueous environment. The average drop size (ignoring the two large ones) is roughly 5 μm . Emulsifiers, although not visible, are present to provide colloidal stability.

The three main ingredients of an emulsion are: bitumen, water, and emulsifier. Bitumen is a complex hydrocarbon that is a by-product of crude oil distillation. The chemical composition of bitumen is highly heterogeneous; it is often broken down into its “SARA” (saturates, aromatics, resins and asphaltenes) fractions. In terms of mechanical properties, bitumen is an extremely viscous material, with viscosity that is typically 10^5 to 10^6 times that of water at room temperature. This viscosity, however, drops rapidly with increasing temperature. For example, the viscosity of a common bitumen used in road building can be 300 Pa·s at 23°C, but falls by 3 orders of magnitude to ~ 0.1 mPa·s at 135°C. Lowering of bitumen viscosity by heating is one of the factors that make emulsification with an aqueous phase achievable. In regard to bitumen’s flow behaviour: it may not be characterizable by a viscosity alone; the material may sometimes be *viscoelastic* — with “visco” meaning liquid-like and “elastic” denoting a solid-like behaviour. Bitumen, which is primarily a viscous liquid, may acquire some elastic character from its larger molecular components such as asphaltenes. A bitumen’s flow behaviour may also be deliberately modified through addition of oil-soluble polymers to enhance its “hardness” (i.e. providing it with more elastic character). A more rigorous discussion of rheology, which is the science of flow and deformation, is found in Chapter 2 of this thesis.

The second component of a bitumen emulsion is water, which typically forms the continuous phase. Before emulsification, the water is typically “softened,” a process in which hard mineral ions (calcium and magnesium) are removed to avoid mineral deposits and other adverse effects. Although not yet fully understood, water chemistry is known to be important to the manufacturing of bitumen emulsions, as well as to its stability during storage.

The last component of a bitumen emulsion is the emulsifier. These are trace amounts of soap-like chemicals (surfactants) that must be added in order for bitumen to be emulsified in

water. Although emulsifiers are present only in very small amounts (often less than 1 wt% in terms of active molecules), they are by far the most important component of an emulsion. The type and dosage of the emulsifier will determine (1) whether the emulsion is oil-in-water or water-in-oil, (2) stability of the emulsion during storage, (3) rate of curing after emulsion application, (4) adhesive strength of the emulsion residue to the aggregates, and (5) rheological behaviour of the emulsion residue. (The main focus of this thesis is on the last feature — the rheological properties of the residue. The first four effects, although equally critical to the performance of an emulsion system, belong in the field of colloid science and will be left for future studies.) The “high-impact” nature of emulsifiers — that so little amount of the substance can have such profound effects — points to the immense opportunities in custom-designing bitumen emulsions through the choice and dosage of emulsifiers. This requires, as a first step, characterization of emulsifiers based on sound scientific principles. For researchers in the pavement industry, the only means to date of characterizing a surfactant is by identifying the charge on the molecule’s polar head group. Thus, a surfactant (i.e. emulsifier) whose head group is negatively charged is said to be *anionic*, while a positively charged head group would make the surfactant *cationic*. This distinguishing feature is also carried over to the classification of bitumen emulsions: an emulsion that is created by anionic surfactants is called an anionic emulsion, and an emulsion created by cationic surfactants is a cationic emulsion. There is strong correlation between the cationic/anionic character of an emulsion and the adhesive strength between its residue and the aggregates (the fourth effect that was mentioned above): more often than not, cationic emulsions will outperform anionics; this is likely due to the Coulombic attraction between the positively charged emulsion drops and the negatively charged mineral surfaces.

Within the broad categories of anionics and cationics, there can be many different types of emulsions (based on the type of surfactant). One special type of anionic emulsion, which is the main focus of this thesis research, is called the *high-float emulsion*.

1.4 High-Float Emulsion

This is a type of emulsion that is known to be especially immune to the problem of “bleeding.” Bleeding, in the pavement industry, refers to the drainage of binder material (the bitumen) from the small spaces between the aggregates (see Figure 1.4). Such an effect will clearly reduce the structural integrity of an asphalt concrete and therefore must be avoided.

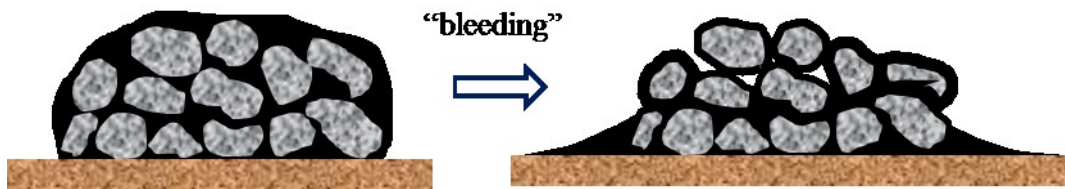


Figure 1.4 “Bleeding” is the drainage of binder material from the small spaces between the aggregates. The strength of the resulting asphalt concrete will clearly be compromised as a result.

The following order-of-magnitude analysis shows that capillary forces alone are not enough to hold the bitumen (assumed for now to be a liquid) in place: Suppose the bitumen has density ρ and surface tension γ . Let h be the thickness of the asphalt concrete layer, and a be the characteristic width of the spacing between the aggregates. If capillary action were the only mechanism of retaining the bitumen between the aggregates, then we must have

$$\rho gh \sim \frac{\gamma}{a} \quad \text{or} \quad a \sim \frac{\gamma}{\rho gh}$$

Putting in typical values of $\gamma \sim 10$ mN/m, $\rho \sim 10^3$ kg/m³, $g \sim 10$ m/s² and $h \sim 1$ cm, we see that the spacing between the aggregates, a , must be of order 100 μ m or smaller. In reality, this spacing is typically ~ 1 mm, which explains the bleeding effect in Figure 1.4 (assuming bitumen

behaves as a liquid). Conversely, if bleeding is absent, it must be due to the presence of additional retaining forces within the binder material.

In regions where the road surface temperature can vary over a wide range, such as in Canada (from -50°C in winter to $+80^{\circ}\text{C}$ in summer), pavement construction is often faced a dilemma: A “softer” bitumen should be used to prevent brittleness and cracking of the asphalt concrete at low temperatures, but the same binder will “bleed” at high temperatures due to its softness. The solution to this dilemma was proposed by McConnaughay (1958), who introduced a special type of anionic emulsion whose residue is resistant to bleeding in the summer and would not be overly brittle in winter; this emulsion had since been called the *high-float emulsion* (a name which appears in the title of this thesis). This peculiar name is derived from a rudimentary test procedure known as the “float test” (ASTM D139); it was designed to quantify a binder’s “consistency.” Briefly, the test involves a floating dish of specific shape, size, material and weight. At the bottom of the dish is a hole, of a specific size, that is plugged with a binder material. The dish is next floated on a 60°C water bath, creating a hydrostatic pressure which pushes on the plugged hole (Figure 1.5).

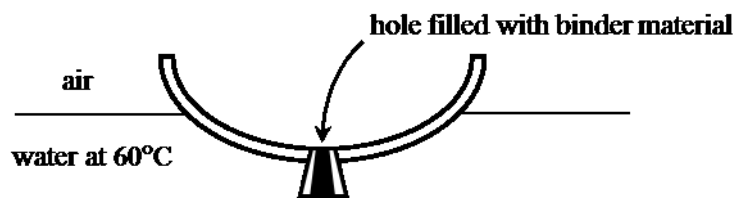


Figure 1.5 The float test (ASTM D139). A binder (either bitumen or the residue of a bitumen emulsion) is used as caulking material as shown. The binder is considered “high-float” if the water breakthrough time is 20 minutes or longer.

The time it takes for the 60°C water to break through the plugged hole is an indication of the binder’s resistance to bleeding. Not surprisingly, a “harder” bitumen would have a longer breakthrough time, which implies a lower tendency to bleed. These binders,

unfortunately, are also the ones that become brittle and crack at sub-zero temperatures. Conversely, softer bitumen, which are designed to remain flexible at low temperatures, would (a) have very short water breakthrough times in float tests, and (b) lead to road surface bleeding at summer temperatures. An exception to this is the *high-float emulsion*. This is an emulsion that is formed using a special type of surfactant (discussed in the next paragraph). When subjected to the float test, the residue of such an emulsion shows a very long — or “high” — breakthrough time; it is for this reason that such emulsions are characterized as “high float.” (The *completely arbitrary* definition of a high-float binder is one whose breakthrough time is 1200 seconds or longer. In practice, this breakthrough time can often be indefinite.) What is remarkable about high-float emulsions is that it can be formed using any — including very “soft” — bitumen. By purposely choosing a soft bitumen (one which normally bleeds at warmer temperatures) to form the droplets, the resulting emulsion residue would have the dual benefit of remaining resilient at cold temperatures and also does not bleed on hot summer days. It is for this reason that high-float emulsions are a popular choice for Canadian road builders.

A high-float bitumen emulsion is formed using a very specific type of anionic emulsifier (not all anionic emulsifiers can lead to high-float quality). The emulsifier is a surfactant that is derived from the saponification of “tall oil” — a by-product from wood pulp mills. (The term “tall oil” comes from the Swedish word “talloja,” which means pine oil. It is manufactured by the Kraft paper process which involves digestion of softwoods with caustic soda and sodium sulphides. The process produces two waste components: rosin and fatty acids, which constitute the crude tall oil or CTO. Saponification of CTO at high pH would yield a tall oil soap, which is

a water-soluble anionic surfactant.) In the pavement industry, it is often claimed that the tall oil soap, when used as emulsifier, can provide the emulsion residue with a “gel-like” quality. A clear demonstration of this gel-like effect is seen in Figure 1.6:



Figure 1.6 Flow behaviours of bitumen (right) and a high-float emulsion residue (left) formed from the same bitumen. The ambient temperature was 23°C.

The can on the right was filled with bitumen; its fluid behaviour was apparent as it slowly drained out of the container over a time scale of hours. The can on the left contained an emulsion residue formed from the *same bitumen*. Although the residue (i.e. what remained after the water component was evaporated from the emulsion) appeared identical to the original bitumen, its rheological behaviour was clearly different. In particular, the residue remained solid-like and showed no sign of deformation under gravity. It is noted that, in general, the “tipped can experiments” in Figure 1.6 correlate perfectly with the (almost equally primitive) float test: a binder that flows out of a tipped can would fail the float test (i.e. water breaking through in less than 1200 seconds), while a “gel-like” material which remains in the can would lead to very long (or “high”) breakthrough times.

Although the flow properties of a high-float emulsion residue are unmistakably different from those of the original bitumen (as evident in Figure 1.6), what have been demonstrated so far are purely qualitative. At present, the only statements that one can make are: whether the

material would flow out of a tipped can, and whether the water breakthrough time in a float test is longer than 1200 seconds. To truly understand the science of high-float emulsions, the following two questions must be answered:

1. What are the true rheological properties of a high-float residue?
2. How does the tall oil soap create these rheological properties?

The focus of this thesis is on the first question.

1.5 The Yield Stress

In many fields of engineering, practitioners have adopted technical terms that are less than precise. The road construction industry, for example, has for many decades used terms such as “hard,” “soft,” and “gel-like” to characterize binder materials. Such adjectives, although descriptive, often lack in scientific rigor. One exception, however, is seen in a paper by Perrone and Sutandar (1980), in which they attributed the “gel-like” behaviour of high-float emulsion residues to a *yield stress*. The yield stress is a well-defined concept in rheology. A material that possesses an intrinsic yield stress will deform as a solid when the externally applied stress is below the yield level, and flow like a liquid when the external stress exceeds the yield (Steffe 1996). Classic examples of materials with yield stresses are tooth paste and mayonnaise — neither will flow out of a container under its own weight (see Figure 1.7). Comparing Figures 1.6 and 1.7, it is clear that although bitumen is a far more “harder” material, it is mayonnaise that has a higher yield stress and, presumably, will be more resistant to bleeding.



$t = 12 \text{ hr}$

Figure 1.7 Mayonnaise has clearly a yield stress. Compared to the bitumen in Figure 1.6, mayonnaise is likely to be more resistant to “bleeding.”

Although Sutandar and Perrone (1980) had alluded to the possibility of a yield stress in high-float emulsion residues, it was no more than a passing comment. A suggestion was made that the yield stress of a high-float residue could be determined using the float test, but no further details were outlined.

1.6 About This Thesis

As mentioned at the end of Section 1.4, this thesis will focus on the rheological behaviour of the high-float emulsion residue. Chapter 2 will be devoted to a brief survey of the relevant principles of rheology. The experimental procedures and an introduction to the dynamic shear rheometer (DSR) will be given in Chapter 3. Chapter 4 will present discussions of the experimental results and their implications; a new rheological model for materials that possess yield stresses will also be proposed. Finally, Chapter 5 will give a summary of the findings of this research and make recommendations for future studies.

Chapter 2: Principles of Rheology — A Brief Summary

Rheology concerns the flow and deformation of materials when they are subjected to external forces. The name “rheology” was first coined by Eugene Bingham, reportedly in the late 1920s (Reiner 1964). Centuries before, however, there were already two branches of physics, known as *fluid mechanics* and *solid mechanics*, which accounted for such phenomena. Fluid mechanics describes how certain materials — specifically, viscous fluids — would flow under applied forces. The distinguishing features of a viscous fluid are:

- it can extend indefinitely when subjected to external load;
- it retains its deformed shape upon removal of the external load; and
- it possesses an inherent property — namely, viscosity — which limits the *rate* at which the material deforms.

Solid mechanics, on the other hand, is concerned with how certain materials — specifically, elastic solids — deform under applied forces. Distinguishing features of an elastic solid are:

- it undergoes finite (often small) deformation when loaded, with the deformation increasing monotonically with the load;
- it returns to its original shape when the external load is removed; and
- it exhibits effectively infinite rates of deformation.

Fluid mechanics and solid mechanics have enjoyed great successes in describing most materials, which surprisingly are well-approximated by one of the above “extreme” behaviours (i.e. elastic solid or viscous liquid). However, as technology advanced, and especially as polymeric materials become more commonplace, it is apparent that there are many situations in which the substance in question behaves neither as an elastic solid nor a viscous liquid; it shows some features of both. For example, some materials are fluid-like in that they can extend indefinitely,

but exhibit partial recoils as the external forces are suddenly removed; other materials can “remember” their original configurations upon removal of external forces, but their rates of deformation are finite. Materials that show both viscous and elastic characteristics are said to be *viscoelastic*; it is the need to understand such materials that led to the science of rheology. In what follows, a brief summary of the principles of rheology will be given. The discussion will not include all detailed (and very mathematical) aspects of rheology and continuum mechanics, but enough to provide a theoretical basis for this present research. More in-depth treatments of the science of rheology can be found in many standard references (e.g. Bird et al. 1987; Malkin & Isayev 2012).

2.1 Stress and Strain

Force (measured in N) and deformation (measured in m) are clearly quantities that are central to the study of rheology. These variables, however, should not be used in the formulation of rheological equations as they are *extensive* measures, i.e. they depend on the size and geometric configuration of the system. A classic example is Hooke’s law for a coil spring, which states that the restoring force in a spring, F , is proportional to its deformation x , i.e.

$$F = kx \tag{2.1}$$

where k is the so-called spring constant (units of N/m). Equation 2.1 applies only to one particular spring size, material and geometric design. Another spring with a slightly different shape or size, even if made of identical material, will have a completely different spring constant. To deal with different springs, one would therefore need a catalogue of all their k values, which can be unnecessarily complex. To avoid this system-specific approach, forces and deformations should be expressed in terms of their *intensive* counterparts (i.e. quantities that do not depend on the size of the system); these are, respectively, *stresses* and *strains*. To be rigorous, stresses and

strains are *tensors*: at every location, the state of stress is expressed by not one — but six — numbers; the same is true for the local state of strain. These two sets of numbers are called the stress tensor and the strain tensor. Stresses and strains need to be expressed as tensors to account for all possible modes of deformation (e.g. bending, twisting, axial extension, etc.). Such an approach is very powerful, but it also involves advanced level mathematics. For simplicity, in this thesis, we focus only on materials that undergo *pure shear* (explained below). Although seemingly restrictive, pure shear deformations will provide sufficient context for a discussion of all forms of material properties; it is also the type of motion that is relevant to the experimental device used in this research, namely, the dynamic shear rheometer (DSR). There is also another advantage to focussing on pure shear deformation: for this type of motion, all but one of the six components — in both the stress tensor and the strain tensor — are zero. As such, we need only deal with one stress component and one strain component; these components are defined below.

Consider a small cubical element of the material that is under study. Pure shear occurs when equal and opposite forces are applied to two opposing faces of the element. It is important to note that these forces act only in tangential directions, i.e. no component of the force is normal to the surface on which it acts. A sketch of the situation is shown in Figure 2.1.



Figure 2.1 An elemental volume of material under pure shear. The differential forces, both of equal magnitude dF , act tangent to the surfaces.

As a result of this shearing, the material element will deform into a “parallelepiped”; this mode of deformation is described as *pure shear*. Figure 2.2 shows the front views of the differential element before and after deformation.

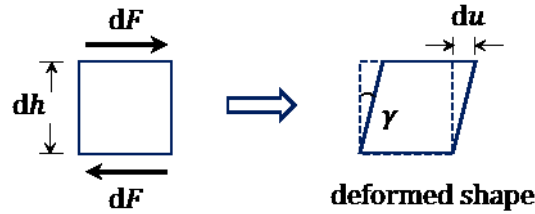


Figure 2.2 Front views of the material element before and after pure shear deformation.

The stress and strain components in a pure shear situation are defined as follows:

$$\text{Shear stress: } \sigma = \frac{dF}{dA} \quad (\text{units of N/m}^2 \text{ or Pa}) \quad (2.2)$$

$$\text{Shear strain: } \varepsilon = \frac{du}{dh} \quad (\text{dimensionless}) \quad (2.3)$$

Since we deal exclusively with shear deformations in this thesis, we will omit the modifier “shear” from here on and refer to σ simply as the stress, and ε simply as the strain. (For small deformations, it is noted that the strain ε is equivalent to the angle γ shown in Figure 2.2; this is why shear strains are often represented as angles of deformation in many textbooks.)

2.2 Rheological Models

Having defined the stress σ and the strain ε , we now need mathematical relations that connect the two. Such relations, which are postulated based on empirical evidence, will describe how a material would deform or flow under applied stresses; these relations are often called *rheological models*. In what follows, the most common rheological models will be reviewed. In addition, based on my own experimental results on high-float emulsion residues (see Chapter 4), it is

necessary to introduce here a new constitutive model that is a Bingham-like fluid with a “soft elastic yield stress” (discussed at the end of this section).

Elastic solid

The first rheological model is that for elastic solids (described at the beginning of this chapter).

In the simplest case, when the stress is proportional to the strain, the material is called a *Hookean solid*; it follows the relation

$$\sigma = G\varepsilon \quad (2.4)$$

where the proportionality constant G is the *shear modulus* (units of Pa). It is noted that while equation 2.4 represents the most common type of elastic behaviour, it is by no means unique. An elastic solid, according to the criteria listed at the beginning of this chapter, can follow any functional relationship between σ and ε as long as (a) $\sigma = 0$ when $\varepsilon = 0$, and (b) the relation does not involve time derivatives of ε (i.e. rates of strain). Figure 2.3a shows the 1-D metaphor of an elastic solid, which is depicted as a coil spring — with the spring force symbolizing the stress, and the spring extension symbolizing the strain.

Viscous fluid

An elastic solid is one that offers resistance to deformation (i.e. ε), but not the *rate* of deformation (i.e. $d\varepsilon/dt$ can be effectively infinite). In contrast, a viscous fluid, as described at the beginning of this chapter, allows only finite $d\varepsilon/dt$ but offers no resistance to any amount of deformation. The simplest rheological model for a viscous fluid is the *Newtonian fluid*, with the stress-strain relation given by

$$\sigma = \mu \dot{\varepsilon} \quad (2.5)$$

where $\dot{\varepsilon}$ is the shorthand notation for $d\varepsilon/dt$ (the rate of strain), and μ is the viscosity (often constant for a given temperature, with units of Pa·s). Viscosity is a mechanism that limits the

rate of deformation through conversion of mechanical energy into heat. Unlike in the case of elastic solids, this mechanical energy cannot be recovered and is said to be *dissipated*. The 1-D metaphor for a viscous liquid is often depicted as a dashpot (see Figure 2.3b), with the tension in the device again symbolizing σ , and the amount of axial extension symbolizing ϵ .

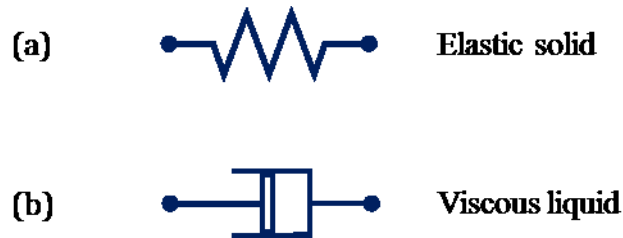


Figure 2.3 One dimensional metaphors of elastic solids and viscous fluids. These are only metaphors as the deformation is not one dimensional (see Figs. 2.1 and 2.2), and of course no springs and dashpots actually exist within the material.

The Hookean solid and Newtonian liquid are the basic rheological models in the fields of solid mechanics and fluid mechanics, respectively. There are, however, many other materials that do not follow these two “extreme behaviours.” Some of the more common examples are discussed in the following.

Kelvin-Voigt solid

This type of material is classified as a solid as it can “remember” its original shape, i.e. it always recoils back to its undeformed configuration upon removal of external forces. However, unlike purely elastic bodies, the rates of deformation of a Kelvin-Voigt material are not infinite; this suggests there is internal dissipation within the material. When subjected to a sudden external load, the material will not deform instantaneously (as does an elastic substance), but will approach its new configuration in a time-dependent (exponential) manner. The simplest way to represent such behaviours is to have an elastic element acting in parallel with a viscous counterpart, as shown in Figure 2.4.

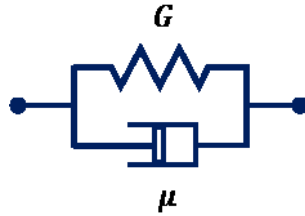


Figure 2.4 Representation of a Kelvin-Voigt material. The elastic element ensures that the material return to its original configuration upon removal of external forces, while the viscous element prevents infinite rates of deformation.

Since the two elements act in parallel, the stress in a Kelvin-Voigt material is the sum of the elastic and viscous contributions, i.e.

$$\sigma = G\varepsilon + \mu\dot{\varepsilon} \quad (2.6)$$

where G and μ are the shear modulus and the viscosity, respectively.

Maxwell fluid

This is a material that flows like a liquid under constant applied force, but exhibits partial recoil when the force is suddenly removed. If subjected to a sudden external load, the Maxwell fluid can deform instantaneously; this aspect is similar to an elastic solid. However, unlike a solid, if the level of strain in a Maxwell fluid is maintained at a fixed level, one will see a gradual (exponential) relaxation of the stress within the material; this continues until σ reaches zero. To model such behaviours, Maxwell (in 1867) suggested putting an elastic element in series with a viscous element, as shown in Figure 2.5.



Figure 2.5 Representation of a Maxwell material. The elastic element is placed in series with a viscous element to capture the phenomenon of internal stress relaxation.

The mathematical model requires that there be two measures of strain within a Maxwell material; these are ε_e and ε_v , which are the strains associated with the elastic element and the viscous element, respectively. Since the elements are in series, the total strain in the material is simply the sum of the two internal parts, i.e.

$$\varepsilon = \varepsilon_e + \varepsilon_v \quad (2.7)$$

Also, the serial arrangement means that the elastic and viscous stresses must be equal:

$$\sigma = G\varepsilon_e = \mu\dot{\varepsilon}_v \quad (2.8)$$

Combining equations 2.7 and 2.8, one gets

$$\dot{\varepsilon} = \frac{\dot{\sigma}}{G} + \frac{\sigma}{\mu} \quad (2.9)$$

where the dots above ε and σ represent differentiations with respect to time.

Materials with yield stress

There is another major class of materials that does not fit any of the above descriptions. These are materials that possess a *yield stress* σ_y , with the following unique features:

- When the magnitude of the applied stress is below σ_y , the material behaves as a solid.
- When the magnitude of the applied stress exceeds σ_y , the material flows like a liquid.

Many substances (e.g. toothpaste, mayonnaise, and the high-float emulsion residue in Figure 1.6) fall into such a category. In the literature, the most general model for materials with yield stresses is the Herschel-Bulkley fluid (Steffe 1996); it is a three-parameter empirical relation of the following form:

$$\left. \begin{array}{l} \text{when } \sigma < \sigma_y : \quad \dot{\varepsilon} = 0 \\ \text{when } \sigma > \sigma_y : \quad \sigma - \sigma_y = K(\dot{\varepsilon})^n \end{array} \right\} \quad (2.10)$$

where K is the so-called “consistency coefficient” and n is the “flow index.” When $n = 1$, the model reduces to the well-known *Bingham plastic*, for which the shear rate $\dot{\epsilon}$ is proportional to the excess stress $\sigma - \sigma_y$. (If $n = 1$ and $\sigma_y = 0$, the material becomes a Newtonian fluid.) It is noted here that the Herschel-Bulkley model (equation 2.10) does not provide a complete description of the rheological behaviour: when $\sigma < \sigma_y$, the material should be allowed to deform as a solid (i.e. with non-zero ϵ), but the elastic stress-strain relation is not specified in equation 2.10. To avoid introducing more empirical parameters, most researchers assume the material to be completely rigid (i.e. $\epsilon = 0$) when the applied stress is below the yield point. This, as we will see in Section 4.3, fails to capture important features of experimental observations. In this thesis, we propose a new three-parameter model (an alternative to the Herschel-Bulkley fluid) for materials that exhibit yield stresses. In our model, the exponent n (associated with viscous dissipation) is fixed at 1; that is, we are neglecting shear-thinning and shear-thickening effects. A new elastic parameter will be added to describe the deformation in the regime $\sigma < \sigma_y$. Our new rheological model is given by

$$\sigma = \sigma_e + \mu \dot{\epsilon} \quad (2.11)$$

where σ_e is the elastic stress, which is a function only of the strain ϵ . Equation 2.11 appears very similar to the Kelvin-Voigt model (cf. eqn 2.6). This similarity in fact points to a subtle but important point: If elastic deformations were allowed below the yield point, one must be careful to not treat the material as purely elastic (implying infinite shear rates). Instead, the material should respond to time-varying excitations in the fashion of a Kelvin-Voigt solid — with finite rates of deformation. Further, the rate-limiting viscosity below the yield point should be the same as that when the yield stress is exceeded. What differentiates equation 2.11 from a Kelvin-Voigt solid is that the elastic stress in this case has two parameters: an elastic modulus G which

determines the initial deformation, and a yield stress σ_y which provides a “ceiling” to the elastic stress (both parameters have units of Pa). The most straightforward way of expressing σ_e in terms of ε is as shown in Figure 2.6a, where

$$\sigma_e = \begin{cases} G\varepsilon; & \varepsilon < \sigma_y/G \\ \sigma_y; & \varepsilon > \sigma_y/G \end{cases} \quad (2.12a)$$

An alternative form for the elastic stress σ_e , which involves also only two parameters, is shown in Figure 2.6b. Here, the elastic function has an initial slope G , which is followed by an exponential (asymptotic) approach to the maximum stress level. In this case, the functional form for σ_e is

$$\sigma_e = \sigma_y [1 - \exp(-G\varepsilon/\sigma_y)] \quad (2.12b)$$

The elastic function in Figure 2.6b (and eqn 2.12b) represents a “softer” elastic response compared to that in Figure 2.6a.

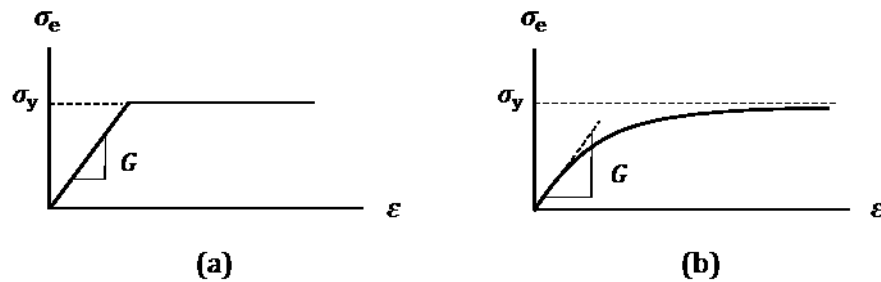


Figure 2.6 The two possible forms of the elastic function $\sigma_e(\varepsilon)$ that appears in equation 2.11. The functional forms in (a) and (b) are given by equations 2.12a and 2.12b, respectively. Both are two-parameter functions, and the elastic stress in case (b) represents a “softer” response.

It will be seen in Section 4.3 that the elastic stress shown in Figure 2.6b provides a much better rheological model for the high-float residue — and most likely also for other materials that exhibit yield stresses. (There is no reason why internal structures which give rise to yield stresses should suddenly “switch off,” as depicted in Figure 2.6a.)

2.3 Response to Time-Varying Excitations

Suppose one is given a material of unknown composition and properties. The best way to probe its rheological behaviour is by subjecting the material to time-varying excitations and observing its response; this is done by either imposing $\varepsilon(t)$ and measuring the resulting $\sigma(t)$, or vice versa. Of all the rheological models discussed in Section 2.2, the most “uninteresting” case is the elastic solid: Since a purely elastic material can undergo infinite rates of deformation, it will react to the applied excitation without any delay or “phase lag.” For example, if an arbitrary time-varying strain $\varepsilon(t)$ is imposed on a Hookean solid (with constitutive relation given by eqn 2.4), the resulting stress will simply be

$$\sigma(t) = G \varepsilon(t) \quad (2.13)$$

Here, the functions $\varepsilon(t)$ and $\sigma(t)$ are exactly in phase and differ only by a factor G (the shear modulus). If, on the other hand, the material has internal dissipation (i.e. viscosity which limits the rates of deformation), its response to time-varying excitations will be considerably more complex, and the response will depend strongly on the rheology of the material. In what follows, two forms of time-varying excitations will be discussed.

Sinusoidal excitation

This is the most common and informative way of characterizing the rheology of a material.

Suppose the time-varying strain $\varepsilon(t)$ is a sinusoidal function given by

$$\varepsilon(t) = \varepsilon_0 \sin(\omega t) \quad (2.14)$$

where ε_0 is the strain amplitude and ω the angular frequency. (The angular frequency is related to T , the period of the oscillation, by the expression $\omega = 2\pi/T$.) In response to this oscillatory excitation, the stress $\sigma(t)$ will, after reaching steady state, also be sinusoidal with the

same frequency ω . However, unlike for elastic solids, the two functions $\sigma(t)$ and $\varepsilon(t)$ will in general be out of phase. The most general form of the stress response is

$$\sigma(t) = \sigma_0 \sin(\omega t + \delta) \quad (2.15)$$

where σ_0 is the stress amplitude and δ is the phase shift. A sketch of this general situation is shown in Figure 2.7.

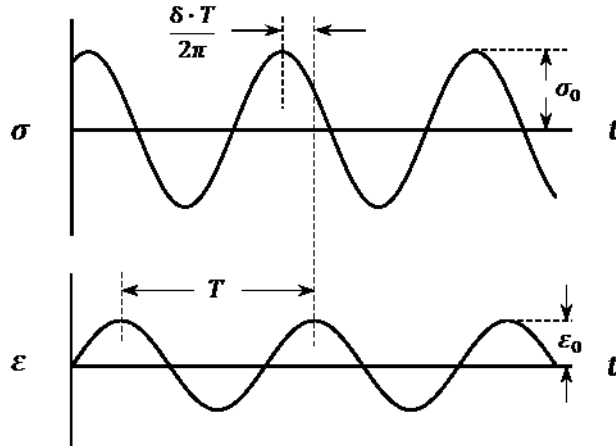


Figure 2.7 Steady state relation between $\sigma(t)$ and $\varepsilon(t)$ when a material is subjected to sinusoidal excitation (with period T). This diagram serves to define the two parameters σ_0/ε_0 and δ . For a linear viscoelastic material, how these two parameters vary with the frequency ω will completely define its rheology.

Equations 2.14 and 2.15 (or alternatively, Figure 2.7) serve as a summary of *all* the information that is needed to uniquely define a material's rheology. To be specific, the two quantities of relevance are the amplitude ratio σ_0/ε_0 and the phase angle δ , both being functions of the frequency ω . In what follows, a few additional quantities will be defined for mathematical convenience. These variables are alternative ways of representing the same information shown in Figure 2.7; they do not provide any new insight into material properties. The first variable is the dynamic shear modulus G^* . It is a complex number with real and imaginary parts G' and G'' , i.e.

$$G^* = G' + iG'' \quad (2.16)$$

where

$$G' = \frac{\sigma_0}{\varepsilon_0} \cos \delta \quad \text{and} \quad G'' = \frac{\sigma_0}{\varepsilon_0} \sin \delta \quad (2.17)$$

From equations 2.16 and 2.17, it follows that

$$|G^*| = \frac{\sigma_0}{\varepsilon_0} ; \quad \tan \delta = \frac{G''}{G'} \quad (2.18)$$

It should be noted that all the above quantities are functions of the frequency ω , with the forms of the functions being unique to the type of material. For example, it can be shown that $\tan \delta$ is proportional to ω for a Kelvin-Voigt solid, and varies as $1/\omega$ for a Maxwell fluid. Indeed, for a material that is linearly viscoelastic (i.e. when the ratio σ_0/ε_0 does not depend on the individual values of σ_0 or ε_0), its rheological character can be *fully specified* by one of the following function pairs:

$$|G^*| = |G^*|(\omega) \quad \text{and} \quad \delta = \delta(\omega)$$

or

$$G' = G'(\omega) \quad \text{and} \quad G'' = G''(\omega)$$

Measurements of these quantities at different values of ω are called “frequency sweeps.”

It is often important to know the amount of mechanical energy that is dissipated (i.e. converted irreversibly to heat) as the material undergoes oscillatory motion. From basic mechanics, the dissipated energy per unit volume (units of J/m^3) over one oscillation is

$$w_d = \int_{t=0}^T \sigma \, d\varepsilon$$

Substituting equations 2.14 and 2.15 into the above expression, one obtains

$$w_d = \pi \sigma_0 \varepsilon_0 \sin \delta \quad (2.19)$$

Using equations 2.17 and 2.19, we can express the imaginary part of G^* (i.e. G'') as

$$G'' = \frac{w_d}{\pi \varepsilon_0^2}$$

For this reason, the quantity G'' (which is a function of ω) is often referred to as the “loss modulus” (i.e. loss of mechanical energy to heat via viscous dissipation).

Another interesting point is that, using the definition $|G^*| = \sigma_0/\varepsilon_0$, the dissipated energy can be written as

$$w_d = \frac{\pi \sigma_0^2}{|G^*|} \sin \delta = \frac{\pi \sigma_0^2}{|G^*|/\sin \delta} \quad (2.20)$$

In the asphalt industry, it has been proposed that to minimize “rutting” (i.e. permanent deformation of asphalt), the dissipated energy w_d should be kept to a minimum. For a given value of σ_0 (presumably reflecting the average weight of a vehicle), w_d can be minimized by maximizing the value of $|G^*|/\sin \delta$; thus, the quantity $|G^*|/\sin \delta$ has become an accepted measure of “rutting resistance.” Although such an index has worked well in the industry, it is argued here that its scientific basis remain dubious. To begin, the parameter $|G^*|/\sin \delta$ is measured at only one frequency (10 rad/s or 1.59 Hz); this provides no information on the material’s rheological character. It is also noted that dissipation is not equivalent to permanent deformation (i.e. rutting), as can be seen from the behaviour of a Kelvin-Voigt material.

Stress-ramp excitation

The other time-varying excitation that will be considered is the “stress-ramp.” Here, the material is subjected to an external stress that increases linearly with time, i.e.

$$\sigma(t) = \alpha t \quad (2.21)$$

where α is the constant ramp rate (units of Pa/s). Such an excitation is aimed specifically at materials with inherent yield stresses. The expectation is that when the applied stress reaches the material’s yield point, there will be obvious and perhaps discontinuous changes to the physical

observables. The observable that is most commonly reported in stress-ramp experiments is the apparent viscosity; it is defined simply as

$$\mu_{\text{app}} = \sigma / \dot{\epsilon} \quad (2.22)$$

and is often plotted against the applied stress (i.e. μ_{app} vs σ , with the latter given by eqn 2.21).

Note that although μ_{app} is what *appears* to be a viscosity, it may not be due to any dissipative mechanism at all. For example, if a stress-ramp were applied to a Hookean solid, it is easy to show that $\mu_{\text{app}} = Gt$, i.e. the apparent “viscosity” increases linearly with time, even though the material is in fact purely elastic and involves no dissipation of energy.

Based on stress-ramp data, plotting μ_{app} vs σ can be a very clear way of separating elastic and viscous effects. It is a simple exercise to show that for (a) a Hookean solid, (b) a Newtonian fluid, and (c) a Bingham plastic, the μ_{app} vs σ relations are as depicted in Figure 2.8. (In the case of Bingham plastic, the material is assumed rigid before the yield point, which gives rise to infinite apparent viscosity for $\sigma < \sigma_y$.)

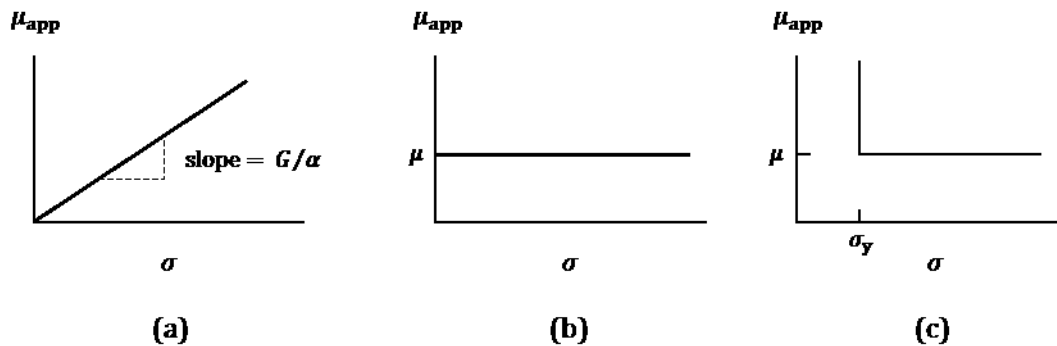


Figure 2.8 Variations of the apparent viscosity μ_{app} with the applied stress σ ; the latter is ramped up linearly with time according to equation 2.21. The three responses are for (a) a Hookean solid, (b) a Newtonian liquid, and (c) a Bingham plastic that is rigid below its yield point.

For materials with more complex rheology, it is very difficult (if not impossible) to determine analytically their responses to stress-ramp excitations. In this thesis, numerical simulations will

be used. Since stress-ramp experiments are intended specifically for materials with yield stresses, we will focus on the two rheological models that we proposed earlier in equations 2.11 and 2.12. Figure 2.9 shows a simple algorithm that is used here to calculate the responses of such materials. Results of this simulation will be discussed in Section 4.3.

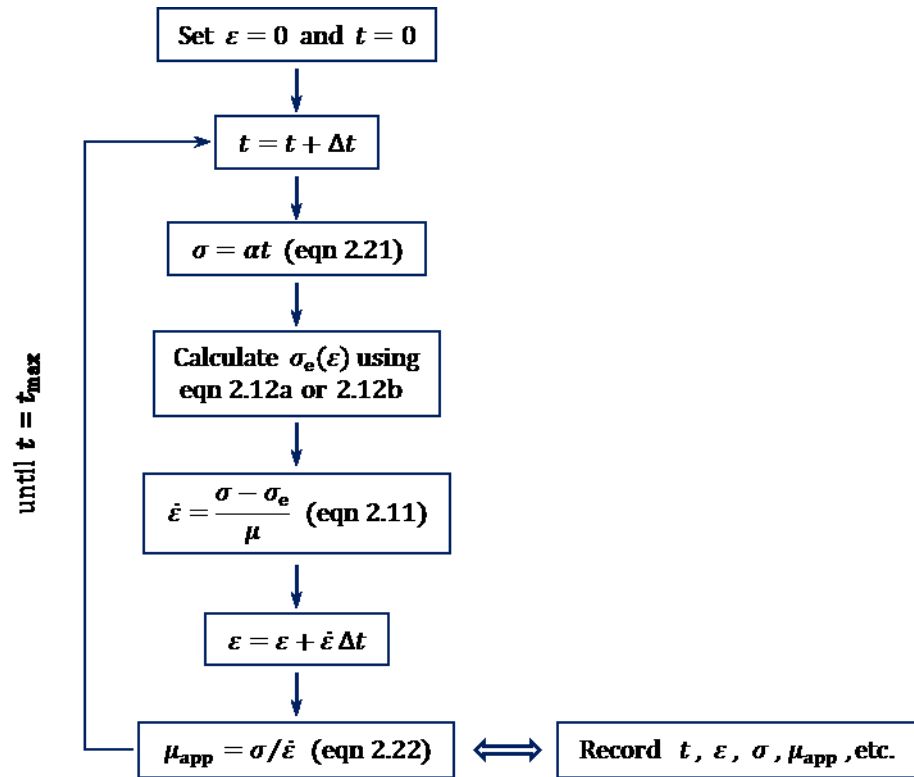


Figure 2.9 Simple algorithm for calculating the response of a material to stress-ramp excitation. The material possesses an inherent yield stress according to equations 2.11 and 2.12.

2.4 Non-uniform Stress and the Dynamic Shear Rheometer

In all of the above discussions, the focus was on *time* dependencies, i.e. only relations between $\sigma(t)$ and $\varepsilon(t)$ were examined. The fact that the stress and the strain were not expressed as functions of position suggested two possible scenarios: (a) they are, at any given time t , uniform over the entire region of interest, or (b) $\sigma(t)$ and $\varepsilon(t)$ should be interpreted as *local*

functions (i.e. at a specific location in space). In view of the experimental setup in this study, the first scenario does not apply: neither σ nor ε can be considered uniform in space, as explained below.

The experimental apparatus used in this study was the dynamic shear rheometer or DSR. In this setup, a sample is placed between two parallel circular plates of radii R ; the plates are separated by a distance h such that $h \ll R$. During experimentation, the bottom plate is fixed and the top plate is rotated by applying a torque T to the shaft; the amount of rotation is measured by the angle Θ as shown in Figure 2.10.

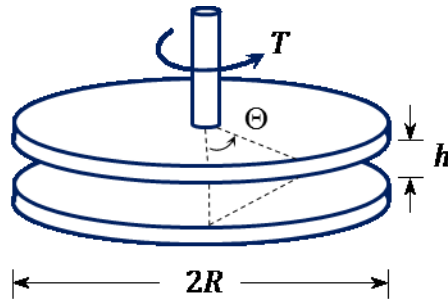


Figure 2.10 Setup of the dynamic shear rheometer (DSR). The torque T is used to calculate the “shear stress” (eqn 2.28), and the angle of rotation Θ is used to calculate the “shear strain” (eqn 2.25).

In DSR experiments, test material that is in contact with a solid surface is known to “stick” to the surface (the “no-slip condition” in fluid mechanics). As such, the infinitesimal layer of sample that is adjacent to the top plate would rotate by an angle Θ , while the layer in contact with the bottom plate would rotate through an angle of zero (i.e. no rotation). For layers in between, it is often *assumed* that the angle of rotation θ would vary linearly between zero and Θ , i.e.

$$\theta = \frac{\Theta z}{h} \quad (2.23)$$

where z is the axial distance from the bottom plate (i.e. $z = 0$ at the bottom plate and $z = h$ at the top plate). It follows from assumption 2.23 that the strain is not uniform, but varies linearly with the radial distance r from the axis of rotation. Specifically, it can be shown that

$$\varepsilon = \frac{\Theta r}{h} \quad (2.24)$$

Equation 2.24 indicates that the strain is zero along the centreline and increases linearly with r until it reaches its maximum value of

$$\varepsilon_{\max} = \frac{\Theta R}{h} \quad (2.25)$$

at the outer rim. Continuing with assumption 2.23, it can be shown that the stress in the sample is also proportional to the radial distance r , i.e.

$$\sigma = \sigma_{\max} \frac{r}{R} \quad (2.26)$$

The quantity σ_{\max} is the maximum stress at the outer rim of the sample. How σ_{\max} relates to deformation will clearly depend on the particular rheological model. For example, for a Kelvin-Voigt solid (see eqn 2.6), it can be shown that

$$\sigma_{\max} = \frac{(G\Theta + \mu\dot{\Theta}) R}{h}$$

Using the above expression, the σ_{\max} for a Hookean solid and for a Newtonian fluid can be determined by simply setting $\mu = 0$ and $G = 0$, respectively.

With equation 2.26, one can now calculate the torque T on the shaft. The general expression for the torque is

$$T = \int 2\pi r^2 \sigma \, dr \quad (2.27)$$

Substituting equation 2.26 into 2.27 gives

$$\sigma_{\max} = \frac{2T}{\pi R^3} \quad (2.28)$$

In commercial shear rheometers, the reported “shear strain” and “shear stress” are often understood to be ε_{\max} and σ_{\max} (i.e. values at the outer rim), and they are calculated from the torque T and the rotation angle Θ using equations 2.28 and 2.25. The shear modulus G (or more generally, $|G^*|$) is obtained from the ratio of σ_{\max} to ε_{\max} :

$$|G^*| = \frac{\sigma_{\max}}{\varepsilon_{\max}} = \frac{2Th}{\pi R^4 \Theta} \quad (2.29)$$

As such, this is consistent with the second scenario that was discussed at the beginning of this section: the time-dependent functions $\sigma(t)$ and $\varepsilon(t)$ are in fact $\sigma_{\max}(t)$ and $\varepsilon_{\max}(t)$. This approach is valid for linear viscoelastic materials such as Hookean solid, Newtonian fluid, Kelvin-Voigt solid and Maxwell fluid (for which the rheological relations have constant coefficients and are linear in ε and/or $\dot{\varepsilon}$). For these materials, assumption 2.23 applies. On the other hand, materials with yield stresses are inherently non-linear (e.g. doubling the applied stress may not necessarily result in 2× the strain and/or 2× the rate of strain). As a result, assumption 2.23 would, strictly speaking, not hold. Nevertheless, given that the gap width between the rotating plates is much smaller than the lateral dimensions (i.e. $h \ll R$ in Figure 2.10), deviations from assumption 2.23 is not expected to be severe. In this study, we will continue to use equations 2.25 and 2.28 to determine stress-strain relations for even materials with yield stresses. The errors associated with this approach are not expected to be large (likely no more than 10 per cent). Investigation of errors due to non-linear rheology (in particular, materials with yield stresses) will require detailed numerical modelling and will be left for future studies.

Chapter 3: Materials and Methods

The experiments in this research, including the float test and dynamic shear rheometry studies, were conducted at Gecan, a division of Canadian Road Builders Inc. (Gecan is a state-of-the-art asphalt testing laboratory located in Acheson, Alberta.) The following is a summary of the procedures involved in sample preparation and testing.

3.1 Materials

Only three types of samples were prepared and subjected to experimentation. The intention here was to focus on the least number of samples that would provide the maximum amount of information and insight. The three materials that were tested were all *binders*, i.e. the glue that holds together the aggregates in an asphalt concrete (see Fig. 1.1). The three binders are:

Binder 1: Bitumen

In all subsequent discussions, we will refer to this material simply as “bitumen.” To be specific, however, this is a special grade of bitumen known as PG 58-28. The designation suggests that the bitumen has certain required physical properties in the temperature range of +58°C to –28°C (McGennis et al. 1994). This particular grade of bitumen was chosen for the present study due to its common usage throughout Alberta — in both road rehabilitation and construction of new pavements. PG 58-28 can be used in a hot-mix process (i.e. liquefaction of bitumen by heating; see Section 1.1) or can form the dispersed phase of an emulsion. It is noted that the bitumen in Figure 1.6 — the material that flowed out of the tin can — was PG 58-28.

Binder 2: Residue A

This is the residue of a high-float emulsion. The proper designation of the emulsion is HF-100S; it is commonly used in Canada for road preservation and rehabilitation. The residue of HF-100S (called “Residue A” in this thesis) is often the binder of choice due to its resistance to

“bleeding.” Most importantly for this study, Residue A is formed from the *same* bitumen as Binder 1 (i.e. PG 58-28). It is noted that the emulsion residue in Figure 1.6 — the material that remained in the tin can — was Residue A. This simple demonstration alone is clear evidence that, contrary to common belief (Fwa 2006), an emulsion residue may *not* necessarily have the same material properties as the original bitumen.

Binder 3: Residue B

Unlike the two former binders, this material is not used in real pavement applications. Residue B is similar to Residue A in every respect, except that it is formed with only *half* of the surfactant dosage. The reason we study such a material is because it is somewhat of a “halfway point” between pure bitumen (PG 58-28, which is prone to bleeding) and Residue A (HF-100S residue, which is resistant to bleeding). As such, Residue B provides an important intermediate case for the fundamental understanding of high-float emulsions.

To summarize, the compositions of the three binders are as follows:

	<u>Bitumen (PG 58-28) wt%</u>	<u>Water wt%</u>	<u>CTO (surfactant) wt%</u>
Bitumen	100	–	–
Residue A’s emulsion	62	35.8	2.2
Residue B’s emulsion	62	36.9	1.1

For the emulsions of Residue A and Residue B, the water component was adjusted to pH 12 with NaOH. Such a high pH was necessary to saponify the CTO (crude tall oil) and allow the release of anionic surfactants into the aqueous phase.

Creation of a bitumen emulsion

In addition to CTO surfactants, which function as emulsifiers, mechanical energy must also be supplied to create a bitumen emulsion. This was done with the aid of a colloidal mill, which is a high shear flow device with an adjustable gap size between its rotor and stator, along with a

variable speed drive to control the shear rate — and ultimately the size of the bitumen droplets. The laboratory colloidal mill used in this study was a Dalworth mill (Figure 3.1). Constructed with a Baldor-Reliancer 5-hp motor, the mill has the capability of rotating at 3450 rpm, creating the necessary mechanical energy to disperse the PG 58-28 bitumen into micron-sized droplets in an aqueous medium. Before being injected into the colloidal mill, the bitumen temperature must be raised to 135°C to decrease its viscosity. The final temperature of the emulsion should, however, be below 100°C to avoid boiling and foaming of the mixture.



Figure 3.1 Colloidal mill at Gecan (in Acheson, Alberta), where experiments were conducted.

From emulsion to residue

With the focus of this study primarily on the residue of high-float emulsions, it is important to note the equipment and procedures associated with obtaining emulsion residues. Currently, there are several accepted methods — the most notable being *residue by distillation* (ASTM D6997/AASHTO T59) testing standards. AASHTO (American Association of State Highway and Transportation Officials) describes this method as a “quantitative determination of residue and oil distillate in emulsified asphalt for specification acceptance, service evaluation, control, and research.” There are also numerous accepted and proposed methods outlined in the

Transportation Research Circular No. E-C122 from 2007, e.g. residue by evaporation (D6934/T59), weathering rack, thermostatically-controlled hot plate, dehydrator and stirred air flow test (SAFT) with nitrogen, to name a few. However, for the present study, residue by distillation was used to obtain the emulsion residues (i.e. Residues A and B); a sketch of this setup is shown in Figure 3.2.

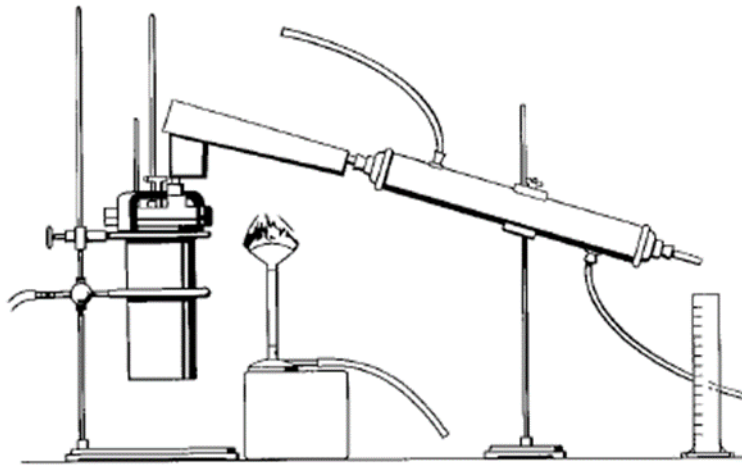


Figure 3.2 Residue-by-distillation set up. This figure was taken from Asphalt Emulsions Manual Series no. 19, developed by AEMA and the Asphalt Institute.

This protocol requires measuring 200 grams of emulsified asphalt into a still, so that the water component can be evaporated off. The duration of the process is approximately one hour and reaching a temperature of 260°C. Distillation is an effective and rapid means of acquiring sufficient residual sample to carry out various tests. As mentioned earlier, although the emulsion residue and the original bitumen are indistinguishable in appearance, they may possess fundamentally distinct rheological properties (as evident in Figure 1.6). The following section provides descriptions of the various methods that were used in this study to probe the rheological properties of the three binders that were mentioned earlier in this section.

3.2 Methods

Two instruments — one rudimentary and the other sophisticated and versatile — were used in this study to test the binder materials. The rudimentary instrument is the float test dish that was illustrated in Figure 1.5; its specific dimensions and related details are summarized in ASTM D139. The sophisticated instrument is the dynamic shear rheometer (DSR) that was depicted in Figure 2.10; the actual make and model of the device are: TA Instruments, Discovery HR-1 Hybrid Rheometer.

The DSR is capable of applying time-varying excitations, in pure shear mode, to a binder sample. The time-varying excitation can be programmed to be of any arbitrary form; however, in this thesis, we will limit our focus to *sinusoidal* and *stress-ramp* excitations (see Section 2.3). For sinusoidal excitation, the two parameters that the experimenter specifies are the strain amplitude ε_0 and the angular frequency ω (equation 2.14).

With the above preamble, the following are the three tests that were performed on the binder materials:

<u>Experiment</u>	<u>Instrument</u>	<u>Description</u>
Float test	Float test dish	Determine water breakthrough time (see Fig. 1.5). Material is deemed “high float” if breakthrough time is longer than 1200 seconds.
Frequency sweep (sinusoidal excitation)	DSR	Fix $T = 58^\circ\text{C}$, $\varepsilon_0 = 12\%$; vary ω from 10 rad/s to 62.83 rad/s. Measure G^* and δ as functions of ω .
Stress-ramp	DSR	Fix $T = 58^\circ\text{C}$; ramp up stress σ linearly with time according to equation 2.21. Measure μ_{app} (equation 2.22) as function of σ .

Chapter 4: Results and Discussions

We now present the results of the three experiments that were described in Section 3.2, following the same order as they were listed.

4.1 Float test

This very crude experiment, designed to measure the “consistency” (a term which has no real rheological meaning) of a binder material, actually provides invaluable guidance to subsequent investigations. Specifically, semi-quantitative results from float tests can give strong hints of whether a material possesses a yield stress — and hence its ability to resist bleeding. Following the exact ASTM D139 procedures, the three binder samples exhibited water breakthrough times as shown below:

<u>Binder</u>	<u>Water breakthrough time (s)</u>
Bitumen	35
Residue A	> 1200 (effectively indefinite)
Residue B	425

The strong contrast is between pure bitumen (i.e. PG 58-28) and Residue A — a high-float residue formed from droplets of the same bitumen. The fact that Residue A showed an indefinite breakthrough time suggests that its “consistency” is not viscosity-based; it is more likely due to an elastic resistance to deformation. This elasticity, however, cannot be Maxwell-like in that it is connected in series to a viscous element (see Figure 2.5): a Maxwell material is capable of unlimited deformation and is therefore likely to fail the float test. The elastic resistance inherent in Residue A must therefore be more akin to Kelvin-Voight-type behaviour (Figure 2.4) as such a material, with its elastic element acting in parallel with dissipation, will allow only finite deformation (and hence maintaining the caulking at the bottom of the floating dish). Residue B,

based on the float test results, appears much more similar to pure bitumen than to Residue A. This is an interesting observation, as Residue B’s composition is almost identical to that of Residue A — except for a reduced amount of surfactants that was used. (Note that the surfactant dosages for Residues A and B were both in trace amounts, but apparently there is a significant difference between “trace amount” and “50% of trace amount”.)

Thus far, we have suggested that (a) there is an inherent elastic component in Residue A, and (b) this elasticity is more in accordance with a Kelvin-Voigt (K-V) solid than a Maxwell fluid. The most direct way of discerning a K-V solid from a Maxwell fluid is from a material’s frequency response. This leads to the next set of experiments.

4.2 Frequency sweep

Recall in Section 2.3, it was mentioned that, depending on whether the material is K-V or Maxwell, the phase angle δ will respond differently to the frequency of oscillation ω ; in particular, $\tan \delta$ is proportional to ω for a K-V solid, and varies as $1/\omega$ for a Maxwell fluid. (Derivation of such a result can be found in any introductory textbook on rheology.)

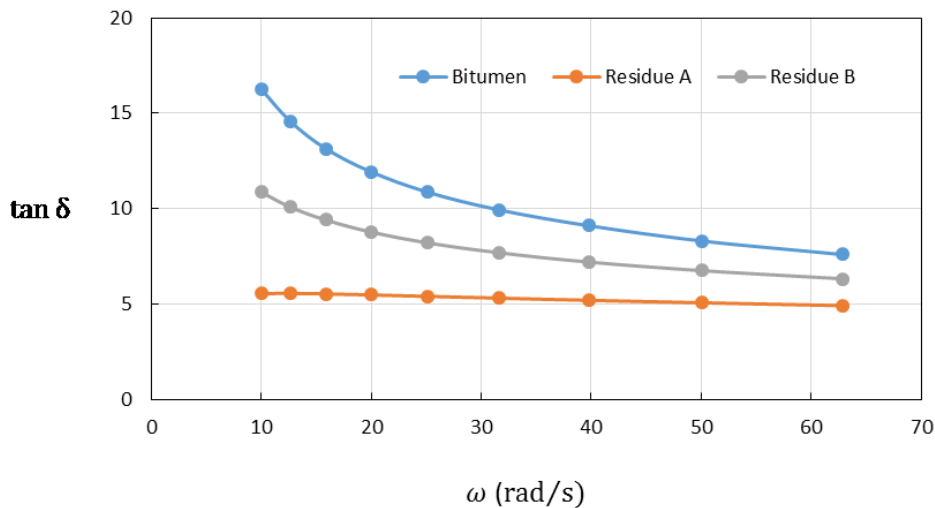


Figure 4.1 Variation of phase angle (i.e. $\tan \delta$) with the frequency of oscillation. The strain amplitude ϵ_0 was 12%.

Figure 4.1 shows the variation of $\tan \delta$ with ω for the three different materials. Although it was only possible to vary the frequency over a narrow range (from 10 to 62.8 rad/s), it is clear that the bitumen sample was behaving most similarly to a Maxwell fluid (i.e. $\tan \delta \propto 1/\omega$). Residue A's frequency response is furthest away from that of a Maxwell fluid. Although one cannot make the case that it is a linear K-V solid (i.e. with $\tan \delta \propto \omega$), it is safe to conclude that *some form of elastic resistance has developed within Residue A*, pushing it closer to becoming a K-V material. Once again, the behaviour of Residue B is intermediate between the other two materials, and much more similar to bitumen.

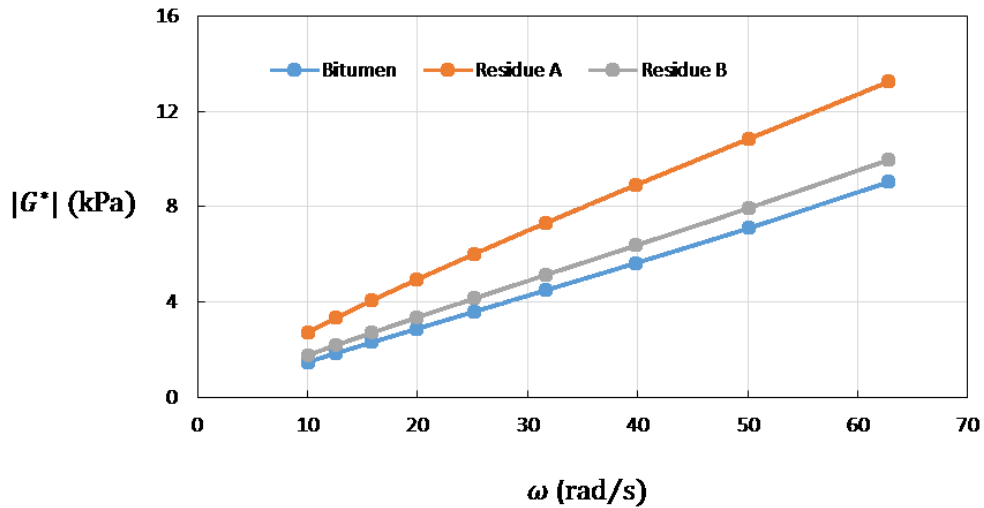


Figure 4.2 Variation of the shear modulus $|G^*|$ with the frequency of oscillation. The strain amplitude ε_0 was 12%.

Based on Figure 4.1 ($\tan \delta$ vs ω), we concluded that some form of elasticity has developed within Residue A. If this were true, it must cause the material to become more resistant to deformation (compared to the original bitumen). Figure 4.2 shows variations of the magnitude of the elastic modulus, denoted $|G^*|$, as functions of ω for the three binders. The parameter $|G^*|$ can loosely be interpreted as a measure of resistance to deformation/flow (lumping together both elastic and viscous effects). As expected, the bitumen binder has the lowest

resistance to deformation/flow, while Residue A has the largest value. The curve corresponding to Residue B is again intermediate between bitumen and Residue A, and much closer to the former.

The above frequency sweep results suggest that Residue A, during its formation, has developed some form of elasticity within its structure. This elasticity acts *in parallel* with the viscosity, making the entire structure resistant to continuous flow — hence the indefinitely long breakthrough time in float tests. One should note, however, that an elasticity acting in parallel with a viscosity does not necessarily make the material a linear Kelvin-Voigt (K-V) solid. Non-linear effects, such as a variable elasticity (see, for example, Figure 2.6), would cause departures from ideal K-V behaviours. The fact that the Residue-A curve in Figure 4.1 does not show simple proportionality between $\tan \delta$ and ω (i.e. straight line through the origin) is therefore not surprising: Hookean elasticity, which is characterized by a constant elastic modulus (equation 2.4), is perhaps the exception rather than the rule for many soft materials.

Based on the results from float tests and frequency sweeps, we strongly suspect that Residue A — the high-float emulsion residue — has an inherent elasticity that is non-linear and acts in parallel with the background viscosity of the bitumen. We further postulate that the non-linear elasticity is characterized by a yield stress σ_y , which is the maximum level of elastic stress created in the material as the body deforms indefinitely (see Figure 2.6). If the externally applied stress is below this yield value, the material deforms as a solid; above the yield stress, it flows like a fluid. To detect the presence of a yield stress, we proceeded to stress-ramp experiments.

4.3 Stress ramp

Details of the stress-ramp experiment were discussed in Section 2.3. The procedure involves applying a constantly-increasing stress to a material this is suspected of having a yield stress. When the applied stress reaches the yield value, there will be an obvious, and perhaps discontinuous, change in the apparent viscosity μ_{app} (see equation 2.22). It is also worth repeating one of the conclusions from Figure 2.8: if the sample were a true Newtonian liquid that does not have a yield stress, we would see $\mu_{\text{app}} = \mu =$ the true viscosity of the material.

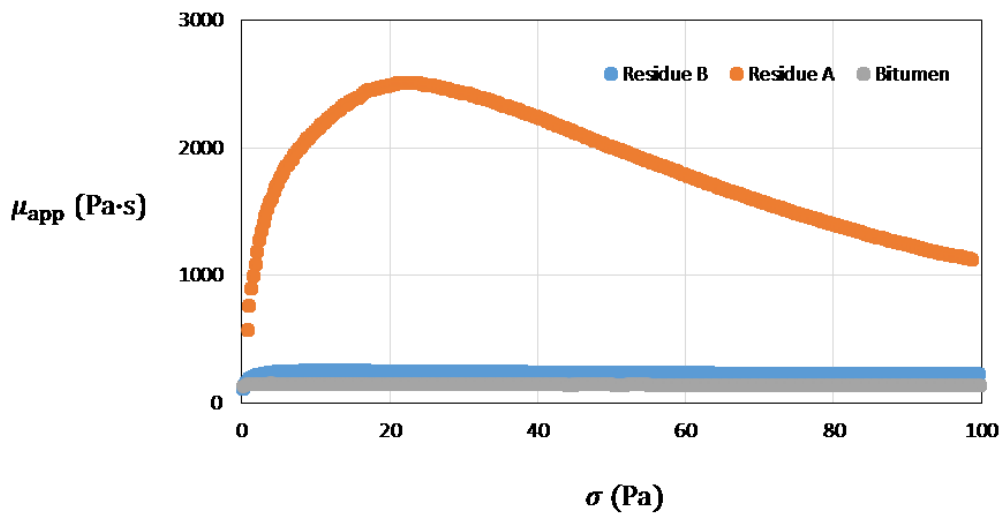


Figure 4.3 Stress-ramp data of the three binder materials. The apparent viscosity of Residue A is seen to peak at $\sigma = 22$ Pa. This value can be interpreted as a rough measure of the yield stress.

Figure 4.3 shows the stress-ramp responses of the three binder materials. The temperature was 58°C , and the ramp rate (α in equation 2.21) was 100 Pa over a period of 1 hour. The bitumen curve showed a constant — and lowest — value of μ_{app} at 140 Pa·s; this is in fact the true viscosity of the substance. The “flatness” of the bitumen curve indicates that this binder does not possess a yield stress. Similarly, the Residue-B curve is essentially level at $\mu_{\text{app}} \approx 220$ Pa·s. This leads one to speculate that Residue B, like bitumen, does not have a yield stress, and that it

is essentially a Newtonian liquid with a viscosity of roughly 220 Pa·s. Interestingly, both bitumen and Residue B had failed the float test (Section 4.1). By contrast, the Residue-A curve shows an obvious peak at $\sigma = 22$ Pa. As will be shown below, such a value can be interpreted as a rough measure of the yield stress. It should also be noted that the very large μ_{app} value for Residue A (up to 2500 Pa·s) is not a real viscosity: As seen in Figure 2.8a, when a Hookean solid is subjected to stress-ramp excitation, the *apparent* viscosity is expected to rise linearly with the applied stress, even though the material has in fact no viscous dissipation at all. This leads one to suggest that, in the case of Residue A, the initial rapid rise in μ_{app} is due not to dissipation, but to an inherent elasticity of the material. As σ reaches the yield value, this elasticity vanishes and hence the subsequent decrease in μ_{app} .

From the above discussion, it is seen the stress-ramp response curve (i.e. μ_{app} vs σ) can be immensely informative. In particular, one can conclude that

- Bitumen (i.e. PG 58-28) is a Newtonian liquid with $\mu = 140$ Pa·s
- Residue B is a Newtonian liquid with $\mu \approx 220$ Pa·s
- Residue A is a complex fluid with a yield stress of roughly 22 Pa

Identifying the yield stress from a μ_{app} vs σ curve is straightforward — one simply needs to locate the peak. However, there are other (more subtle) properties of a yield-stress material, such as the elastic modulus, which should also be determined (see equations 2.11 and 2.12). To further understand these subtle features would require detailed numerical modelling.

Numerical simulation of stress-ramp excitation

With the aid of a computer, it is relatively straightforward to simulate the stress-ramp curve — provided a rheological model is given. In Section 2.2, we had proposed two such models for yield-stress materials. These models are specified by equations 2.11 and 2.12; the elastic stresses

associated with these models are illustrated in Figure 2.6. Both these models involve three parameters: the yield stress σ_y , the elastic modulus G , and the viscosity μ . In addition, the stress ramp rate α must also be specified. Given these values, the stress-ramp response can be calculated using the algorithm shown in Figure 2.9.

After some trial simulations, it became clear that the first yield-stress model — the one whose elastic stress is illustrated in Figure 2.6a — is completely unrealistic. The second yield-stress model, with the “softer” elasticity as shown in Figure 2.6b, provides a much better approximation to the observed trend. As demonstration, we will show two simulations based on the following parametric values:

$$\sigma_y = 30 \text{ Pa}; \quad G = 6 \text{ Pa}; \quad \mu = 500 \text{ Pa}\cdot\text{s}; \quad \alpha = 100 \text{ Pa}/3600 \text{ s}$$

First, using the elastic stress according to equation 2.12a (and illustrated in Figure 2.6a), we have the following stress-ramp response:

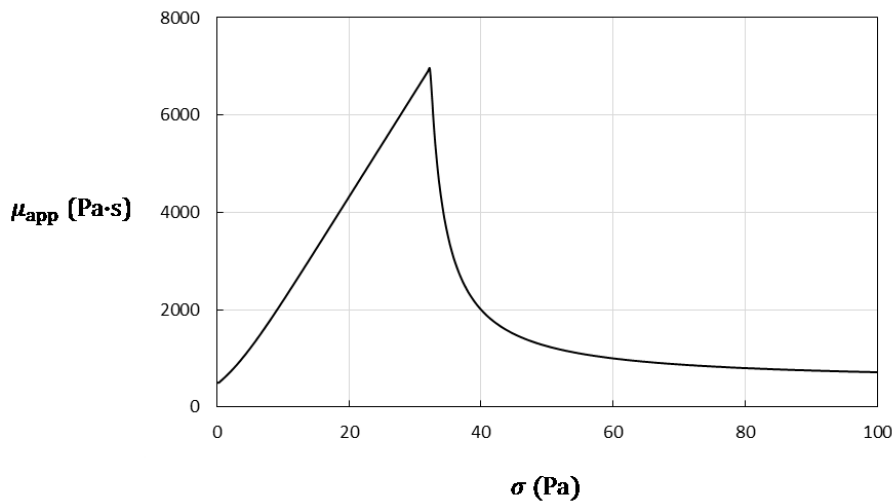


Figure 4.4 Numerical simulation of stress-ramp response according to equations 2.11 and 2.12a.

Comparing this calculated curve with the Residue-A curve in Figure 4.3, it is clear that this rheological model is unrealistic. The problem is due to the abrupt change in elastic modulus (i.e. slope of the σ_e vs ϵ curve in Figure 2.6a), which leads to the pointed peak in Figure 4.4. In

contrast, the elastic model according to equation 2.12b (and illustrated in Figure 2.6b) produced the following curve:

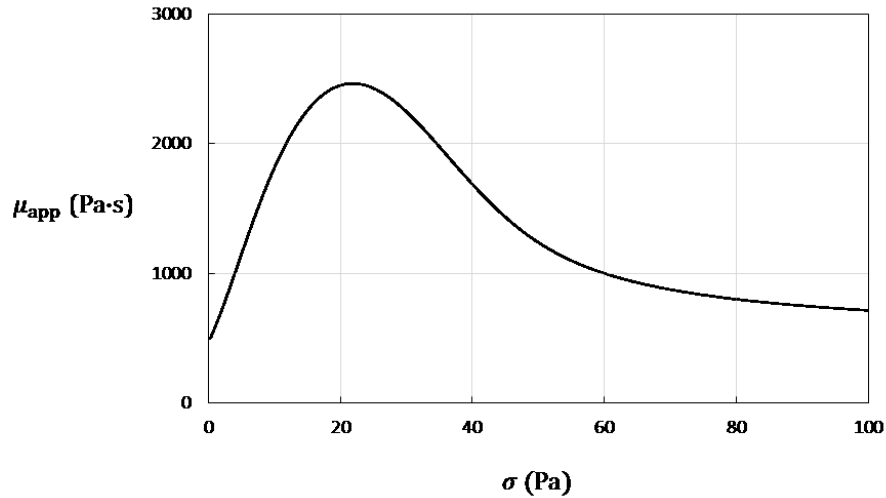


Figure 4.5 Numerical simulation of stress-ramp response according to equations 2.11 and 2.12b.

Although not exactly the same as the Residue-A curve in Figure 4.3, the “softer” elastic model represents a significant improvement over what is shown in Figure 4.4. It is noted that this improvement was not made at the expense of additional parameters — both models involved three fitting values.

Chapter 5: Conclusions and Future Work

We have demonstrated that the high-float emulsion residue (Residue A) has rheological properties that are completely different from those of the original bitumen (PG58-28). Most importantly, the material possesses a yield stress which can prevent the “bleeding” problem that was illustrated in Figure 1.4. The yield stress of the high-float residue is estimated to be about 22 Pa. We have also proposed a new rheological model (equations 2.11 and 2.12b) which best captures the flow properties of the high-float emulsion residue.

This thesis has made significant contributions toward understanding the rheology of high-float residues. In addition to proposing a new yield-stress model, we have also demonstrated that a simple protocol — the stress-ramp excitation — can be used to determine yield stress values. With further development, such a procedure can have the potential of replacing the traditional float test (ASTM D139).

This research was focussed entirely on the rheological aspects of high-float residues. What is clearly missing is a basic understanding of how the yield stress and the inherent elasticity are created in the material. Such a mechanistic study would involve principles of colloid science and a careful examination of the microstructure of the emulsion residue; this will be left for future work.

References

1. AEMA, 2016. <http://www.aema.org/resources/faqs/basics-of-asphalt-emulsions/>
2. Al-sabagh, A. The Relevance HLB of surfactants on the Stability of Asphalt emulsion. Elsevier Science B.V. 2002, Colloids and Surfaces A: Physicochemical and Engineering Aspects 204, 73-83.
3. Alberta Transportation, Specification for High Float Emulsified Asphalts, Section 5, ASPH-9 (Alberta Transportation, 1986).
4. American Association of State Highway and Transportation Officials (AASHTO). Standard Specifications for Performance-Graded Asphalt Binder. AASHTO Designation M320-10 Table 1. Standard Specifications for Transportation Materials and Methods of Sampling and Testing, 32nd Edition. (AASHTO, 2012).
5. Anderson, Michael R. The Asphalt Handbook. Asphalt Institute Manual Series no. 4 (MS-4). Chapter 2: Petroleum Asphalt, Section 2.3 Dominant Practice: Performance Graded, 2007.p 49-53
6. Asphalt Binder Testing. Asphalt Institute. Manual Series No. 25 Third Edition, 2012
7. Asphalt Emulsions. AEMA, Asphalt Institute. A Basic Asphalt Emulsion Manual. Manual Series No. 19 Third Edition.
8. Asphalt Emulsion Technology, Review of Asphalt Emulsion Residue Procedures. Transportation Research Circular No. E-C122, 2007
9. ASTM D244-09, Standard Test Methods and Practices for Emulsified Asphalts, ASTM International, West Conshohocken, PA, 2009, www.astm.org
10. ASTM D6373-15, Standard Specification for Performance Graded Asphalt Binder, ASTM International, West Conshohocken, PA, 2015, www.astm.org
11. ASTM D6934-08, Standard Test Method for Residue by Evaporation of Emulsified Asphalt, ASTM International, West Conshohocken, PA, 2008, www.astm.org
12. ASTM D6997-12, Standard Test Method for Distillation of Emulsified Asphalt, ASTM International, West Conshohocken, PA, 2012, www.astm.org
13. ASTM D7175-15, Standard Test Method for Determining the Rheological Properties of Asphalt Binder Using a Dynamic Shear Rheometer, ASTM International, West Conshohocken, PA, 2015, www.astm.org
14. Banerjee, A.; Bhasin, A.; Prozzi, J. Characterizing stability of Asphalt Emulsions Using Electrokinetic Techniques. Journal of Materials in Civil Engineering 2013, 25, 78-85.
15. Berg, J. An Introduction to Interface and Colloids: The Bridge to Nanoscience, 2010. World Scientific Publishing Co. Pte. Ltd. 25-26, 148-166.

16. Bird, R.B., Armstrong, R.C. and Hassager, O. *Dynamics of Polymeric Liquids, Volume 1: Fluid Mechanics*, 2nd edition, Wiley (1987).
17. Environment Canada, Possible Control Measures on Volatile Organic Compounds (VOC) Concentration Limits in Cutback Asphalt and Emulsified Asphalt. Discussion Paper and Considerations. Her Majesty the Queen in Right of Canada, represented by the Minister of the Environment, 2013.
18. Johnson, R. and Juristovski, A. Physical Properties of Tall Oil Pitch Modified Asphalt Cement Binders. ASTM STP 1241. American Society for Testing and Materials, Philadelphia, 1995.
19. Maki, K., Renardy, Y. The Dynamics of a Viscoelastic Fluid Which Displays Thixotropic Yield Stress Behaviour. *Journal of Non-Newtonian Fluid Mechanics*. Volumes 181-182, August 2012, p. 30-50.
20. Malkin AY, Isayev A. Rheology: Concepts, Methods and Applications (2nd ed.), ChemTec Publishing, Toronto (2012).
21. McConnaughay, K. Asphaltic Paving Composition, US Patent 2,855,319. United States Patent Office. Patented Oct. 7, 1958.
22. McGennis RB, Shuler S, Bahia HU. “Background of SUPERPAVE Asphalt Binder Test Methods”, Report No. FHWA-SA-94-069, Federal Highway Administration, Washington, D.C. (1994).
23. McNichol, D. (2005). *Paving the Way: Asphalt in America*. National Asphalt Pavement Association; Lanham, Maryland.
24. Perrone, P., Sutandar, T. High Float Emulsified Asphalt; It’s Properties, and Applications. Canadian Technical Asphalt Association 1980. p 80-107.
25. Redilius, P. and Walter J. Emulsion and Emulsion Stability. Chapter 11: Bitumen Emulsions. Taylor and Francis Group, LLC. 2006.
26. Reiner M. “The Deborah Number” *Physics Today* 17(1) 62 (1964).
27. Scientific American ‘Asphalt Emulsion Finds Uses’ April 1930, Vol. 142, p 316.
28. Steffe James F. Rheological Methods in Food Processing Engineering, Freeman Press, East Lansing, MI, USA (1996).
29. Transport Canada, 2016. <https://www.tc.gc.ca/eng/policy/anre-menu-3021.htm>
30. Understanding Rheology of Structured Fluids. TA Instruments, 2016. http://www.tainstruments.com/pdf/literature/AAN016_V1_U_StructFluids.pdf